HHS Public Access

Author manuscript

*J Mol Histol*. Author manuscript; available in PMC 2019 July 17.

Published in final edited form as:

*J Mol Histol*. 2017 April ; 48(2): 83–98. doi:10.1007/s10735-016-9708-x.

# Inactivation of bone morphogenetic protein 1 (*Bmp1*) and tolloid-like 1 (*Tll1*) in cells expressing type I collagen leads to dental and periodontal defects in mice

**Hua Zhang**[1], **Priyam Jani**[1], **Tian Liang**[1], **Yongbo Lu**[1], and **Chunlin Qin**[1]

[1]Department of Biomedical Sciences and Center for Craniofacial Research and Diagnosis, Texas A&M College of Dentistry, 3302 Gaston Ave., Dallas, TX 75246, USA

## Abstract

Bone morphogenetic protein 1 (BMP1) and tolloid-like 1 (TLL1) belong to the BMP1/tolloid-like proteinase family, which cleaves secretory proteins. The constitutive deletion of the *Bmp1* or *Tll1* genes causes perinatal or embryonic lethality in mice. In this study, we first studied the β-galactosidase activity in mice in which an IRES-lacZ-Neo cassette was inserted in the intron of either the *Bmp1* or the *Tll1* gene; the β-galactosidase activities were used to reflect the expression of endogenous *Bmp1* and *Tll1*, respectively. Our X-gal staining results showed that the odontoblasts in the tooth and cells in the periodontal ligament express both *Bmp1* and *Tll1*. We then created $Bmp1^{flox/flox}$ and $Tll1^{flox/flox}$ mice by removing the IRES-lacZ-Neo cassette. By breeding *2.3 kb Col1a1*-Cre mice with the $Bmp1^{flox/flox}$ and $Tll1^{flox/flox}$ mice, we further generated *Col1a1*-Cre;$Bmp1^{flox/flox}$;$Tll1^{flox/flox}$ mice in which both *Bmp1* and *Tll1* were inactivated in the Type I collagen-expressing cells. We employed X-ray radiography, histology and immunohistochemistry approaches to characterize the *Col1a1*-Cre;$Bmp1^{flox/flox}$;$Tll1^{flox/flox}$ mice. Our results showed that the molars of the *Col1a1*-Cre;$Bmp1^{flox/flox}$;$Tll1^{flox/flox}$ mice had wider predentin, thinner dentin and larger pulp chambers than those of the normal controls. The dentinal tubules of the molars in the *Col1a1*-Cre;$Bmp1^{flox/flox}$;$Tll1^{flox/flox}$ mice appeared disorganized. The level of dentin sialophosphoprotein in the molars of the 6-week-old *Col1a1*-Cre;$Bmp1^{flox/flox}$;$Tll1^{flox/flox}$ mice was lower than in the normal controls. The periodontal ligaments of the *Col1a1*-Cre;$Bmp1^{flox/flox}$;$Tll1^{flox/flox}$ mice were disorganized and had less fibrillin-1. Our findings indicate that the proteinases encoded by *Bmp1* and *Tll1* genes play essential roles in the development and maintenance of mouse dentin and periodontal ligaments.

### Keywords

Bone morphogenetic protein 1; Tolloid-like 1; Knockout mice; Tooth; Periodontium; Type I collagen

✉Yongbo Lu, ylu@tamhsc.edu; Chunlin Qin, cqin@tamhsc.edu.

## Introduction

The proteolytic processing of extracellular matrix (ECM) proteins is essential to organogenesis. The bone morphogenetic protein 1 (BMP1)/mammalian tolloid-like proteinase family is one category of astacin proteinases that plays critical roles in processing proteins secreted into the ECM (Hopkins et al. 2007; Sterchi et al. 2008; Muir and Greenspan 2011). The BMP1/tolloid-like proteinase family includes four members: BMP1, tolloid (TLD), tolloid-like 1 (mTLL1) and tolloid-like 2 (TLL2). TLD is a longer splice variant transcribed from the same gene that encodes BMP1 (Takahara et al. 1994; Reynolds et al. 2000). BMP1/TLD is initially synthesized as a zymogen with an N-terminal prodomain, and the removal of the prodomain in the *trans*-Golgi network (TGN) activates this zymogen. The activation of BMP1 occurring inside the cells suggests that this proteinase may cleave its substrates prior to the secretion of the secretory proteins to the ECM (Leighton and Kadler 2003). While all four members are expressed in the mouse gastrulas, their expression profiles show remarkable divergence after the gastrula stage (Scott et al. 1999; Muir and Greenspan 2011). Mouse BMP1 and TLD are expressed in a variety of tissues including bone at the late stage of embryonic development and after birth (Suzuki et al. 1996; Scott et al. 1999; Muir and Greenspan 2011). *Bmp1*$^{-/-}$ mice are perinatally lethal (Suzuki et al. 1996). The expression of mouse TLL1 is limited to the cardiovascular system until 10 days post coitum (dpc) (Clark et al. 1999). After 10 dpc, TLL1 shows a broad expression profile (Scott et al. 1999; Clark et al. 1999; Muir et al. 2014). The *Tll1*$^{-/-}$ mice are embryonically lethal (Clark et al. 1999). TLL2 is specifically expressed in the skeletal muscle of mice after gastrulation (Scott et al. 1999); the homozygous *Tll2*-null mice have a small reduction in muscle mass with a normal skeleton (Lee 2008).

The proteinases in the BMP1/tolloid-like family are believed to cleave and activate a number of proteins including several types of procollagen, prolysyl oxidase, gliomedin, laminin 5, perlecan, probiglycan, latent TGF-beta binding proteins, osteoglycan, chordin, myostatin, dawdle, activin, dentin matrix protein 1 and dentin sialophosphoprotein (Steiglitz et al. 2004; Hopkins et al. 2007; Von Marschall and Fisher 2010; Muir and Greenspan 2011). In vitro studies have indicated that the four members of this proteinase family may have redundant roles in cleaving/activating ECM proteins (Steiglitz et al. 2004; Von Marschall and Fisher 2010; Muir and Greenspan 2011; Ritchie et al. 2010). The cleavage/activation of certain ECM proteins by the BMP1/tolloid-like family is believed to play important roles in the normal development of connective tissues such as bone and dentin (Steiglitz et al. 2004; Von Marschall and Fisher 2010; Muir et al. 2014; Zhu et al. 2012a, b). Previous studies have shown the co-expression of *Bmp1* and *Tll1* in bone (Scott et al. 1999; Muir et al. 2014). While there have been reports regarding the expression of *Bmp1* in the pulp-predentin-dentin complex (Tsuchiya et al. 2011; Muromachi et al. 2015), there are no reports regarding the expression of *Tll1* in the cells of dental tissues. There are also no reports about the expression of *Bmp1 or Tll1* in the periodontal ligaments (PDL). A previous study reported that the conditional knockout of both *Bmp1* and *Tll1* by tamoxifen-inducible Cre recombinase driven by the human ubiquitin C promoter resulted in osteogenesis imperfecta in mice (Muir et al. 2014). Many factors, including genetic alterations and changes in

nutrition may affect dentin and/or periodontal tissue development (Li and Zhang 2015; Yang et al. 2016; Ye et al. 2016; Zhou et al. 2016). However, there has been no report about the effects of *Bmp1*- or *Tll1*-deficiency on dental or periodontal tissues. We recently created mice in which both *Bmp1* and *Tll1* were inactivated in Type I collagen-expressing cells, which include odontoblasts in the tooth and fibroblasts in the periodontal ligament. In this study, we analyzed the expression of *Bmp1* and *Tll1* in the dental and periodontal tissues and characterized the teeth and periodontium in the mice with the double conditional deletion of these genes.

## Materials and methods

### Generation of *Bmp1*-floxed and *Tll1*-floxed mice

The *Bmp1* mutant mouse strain used to create the *Bmp1*-floxed mice was created from ES cell clone EPD0694_1_B05 generated by the Wellcome Trust Sanger Institute and made into mice in the Knockout Mouse Project (KOMP) Repository (http://www.komp.org) and the Mouse Biology Program (http://www.mousebiology.org) at the University of California Davis. The mutant allele, named $Bmp1^{tm1a(KOMP)Wtsi}$ is the *Bmp1*-targeted knockout first allele with conditional potential. As shown in Fig. 1a, a reporter *LacZ* gene (encoding β-galactosidase) flanked by two flippase recognition target (FRT) sites was inserted into intron 6; the region from exon 7 through exon 8 was flanked by two loxP sites. The mutant alleles of F1 agouti mice were genotyped by polymerase chase reaction (PCR) analyses (Fig. 1b). We referred to the mice with one allele of $Bmp1^{tm1a(KOMP)Wtsl}$ (i.e., targeted *Bmp1* allele in Fig. 1a) as $Bmp1^{lacZ\text{-}flox/+}$ mice. These mice were intended to be used for X-gal staining to investigate the expression pattern of *Bmp1*. To produce the conditional allele $Bmp1^{flox}$, the $Bmp1^{lacZ\text{-}flox/+}$ mice were crossed with the FLP mouse line to remove the IRES-lacZ-Neo cassette. The mice with one allele of *Bmp1* floxed by two loxP sites without the IRES-lacZ-Neo cassette (i.e., floxed *Bmp1* allele in Fig. 1a) were designated as $Bmp1^{flox/+}$ mice. The $Bmp1^{flox/+}$ mice were inbred to create $Bmp1^{flox/flox}$ mice. The $Bmp1^{flox/+}$ and $Bmp1^{flox/flox}$ alleles were identified by PCR (Fig. 1c).

To create the *Tll1*-floxed mice, we purchased two correctly targeted ES cell clones (EPD0631_4_ D01 and EPD0631_4_ H02; allele name: $Tll1^{tm1a(EUCOMM)Wtsi}$) from the European Conditional Mouse Mutagenesis Program (EUCOMM) Repository (http://www.eummcr.org). The mutation allele is a *Tll1*-targeted knockout first allele with conditional potential. As shown in Fig. 1d, an IRES-lacZ-Neo cassette flanked by two FRT sites was inserted into intron 3; the region from exon 4 through exon 5 was flanked by two loxP sites. The ES clones were injected into the blastocysts of C57 BL/6 mice in the Transgenic Core Facility at the University of Texas Southwestern Medical Center, Dallas. Male chimeras were crossbred with C57BL/6 females to produce F1 agouti offspring. The mutant alleles of the F1 agouti mice were genotyped by PCR analyses (Fig. 1e). We referred to the mice with one allele of $Tll1^{tm1a(EUCOMM)Wtsi}$ as $Tll1^{lacZ\text{-}flox/+}$ mice. These mice were to be used for X-gal staining to investigate the expression pattern of *Tll1*. To produce the conditional allele $Tll1^{flox}$, the $Tll1^{lacZ\text{-}flox/+}$ mice were crossed with the FLP mouse line to remove the IRES-lacZ-Neo cassette. The mice with one allele of *Tll1* that was floxed by two

loxP sites without the IRES-lacZ-Neo cassette were designated as *Tll1*$^{flox/+}$ mice, which were inbred to generate *Tll1*$^{flox/flox}$ mice.

The targeted and floxed alleles were identified by PCR analyses of genomic DNA extracted from tail biopsy tissues using specific primers (Table 1); the positions of these designed primers are illustrated in Fig. 1a, d.

## Generation of double conditional *Bmp1*- and *Tll1*-knockout (dcKO) mice

We crossed the mice carrying the *2.3 Col1a1*-Cre transgene (Liu et al. 2014) with the *Bmp1*$^{flox/flox}$;*Tll1*$^{flox/flox}$ mice to generate *2.3 Col1a1-Cre;Bmp1*$^{flox/fox}$;*Tll1*$^{flox/flox}$ ("double conditional *Bmp1*- and *Tll1*-knockout" or "dcKO") mice. The excision of the floxed *Bmp1* exons 7 and 8 by Cre recombinase results in the removal of a stretch of 241 nucleotides that encode the C-terminal region of the zinc binding activity site in the astacin domain shared by both BMP1 and TLD (Hopkins et al. 2007; Muir and Greenspan 2011). This also leads to a reading-frame shift in the BMP1 mRNA. Thus, the *Bmp1*$^{\Delta 7\text{-}8}$ allele is essentially null because the resulting mRNA encodes a truncated protein with 256 amino acids, which lacked an active zinc binding site and should be nonfunctional. The excision of floxed-*Tll1* exons 4 and 5 results in the removal of a stretch of 271 nucleotides that encode the N-terminal region of the active zinc binding site in the astacin domain (Hopkins et al. 2007; Muir and Greenspan 2011) and also cause a reading-frame shift in the TLL1 mRNA, leading to a premature stop codon. The *Tll1*$^{\Delta 4\text{-}5}$ allele produces an mRNA encoding a truncated protein with 90 amino acids, which would be unlikely to function.

Genotyping for the Cre transgene was carried out by PCR analyses using primers Cre-F: 5′-CCCGCAGAACCTGAAGATG-3′ and Cre-R: 5′-GACCCGGCAAAACAGGTAG-3′, as previously reported (Liu et al. 2014). Specific primers (Table 1) were designed to detect the *Bmp1*$^{\Delta 7\text{-}8}$ or *Tll1*$^{\Delta 4\text{-}5}$ alleles generated after the Cre recombination event. As shown in Fig. 1c, Bmp1 F and R primers generated a 615-bp fragment for the *Bmp1*$^{\Delta 7\text{-}8}$ allele; in Fig. 1f, Tll1 5′am and loxP primers produced a 270-bp fragment for the *Tll1*$^{\Delta 4\text{-}5}$ allele. The age- and sex-matched littermate mice lacking the Cre transgene were used as normal controls in this study.

All the animal procedures were performed in accordance with the National Institutes of Health Guide for the Care and Use of Laboratory Animals and approved by the Institutional Animal Care and Use Committee of Texas A&M College of Dentistry (Dallas, TX, USA).

## X-Gal staining

For X-Gal staining of the newborn mouse samples, the half heads dissected from the *Bmp1*$^{lacZ\text{-}flox/+}$ and *Tll1*$^{lacZ\text{-}flox/+}$ mice were fixed in 4% ice-cold paraformaldehyde (PFA) in phosphate-buffered saline (PBS) (pH 7.4) for 30 min on a shaker and washed with PBS solutions. The samples were then processed for sucrose infiltration, and 10 μm serial frozen sections were prepared with a cryostat microtome. The frozen sections were stained in standard X-Gal (Gold Biotechnology, St. Louis, MO, USA) solution for 36 h at 37 °C in the dark and counterstained with Nuclear Fast Red.

The mandibles from 4- or 5-week-old mice were dissected free of the soft tissues, fixed in 4% ice-cold PFA for 1 h on a shaker and washed with PBS solutions. The mandibles were then decalcified in 15% ethylenediaminetetraacetate (EDTA) solution (pH 7.4) at 4°C for 5–7 days. The samples were incubated in standard X-Gal solution for 36 h at 37 °C in the dark followed by dehydration using alcohol and embedded in paraffin. Sections were cut to a 10-μm thickness and counterstained with Nuclear Fast Red.

## X-ray radiography

The mandibles dissected from 3- and 6-week-old control and dcKO mice were analyzed using an X-ray radiography system (Faxitron MX-20DC12 system; Faxitron Bioptics, Tucson, AZ, USA). Based on the X-ray radiographs of the 6-week-old mouse mandibles, we measured the dentin thickness at the cervical region of the first mandibular molars using ImageJ software. We also measured the mesial and distal root length of these molars. The data obtained from five samples per group were used for the quantitative analyses.

## Microcomputed tomography (μCT)

The mandibles dissected from 6-week-old control, *Col1a1*-Cre;$Bmp1^{flox/flox}$;$Tll1^{flox/+}$, *Col1a1*-Cre;$Tll1^{flox/flox}$;$Bmp1^{flox/+}$ and dcKO mice were examined by μCT (Scanco μCT35 imaging system; Scanco Medical, Brüttisellen, Switzerland) with a low-resolution scan (20 μm slice increment) for overall morphological assessment. Following these evaluation, a high-resolution scan in 3.5 μm slice increments was performed on 6-week-old control and dcKO mouse samples to examine the mandibular first molars. The morphometric parameter analysis was performed using the built-in software of the μCT system. The dentin volume (DV), total tissue volume (TV, the sum of the dentin and pulp volume), dentin apparent density (averaged mineral density over the total tissue volume) and material density (dentin mineral density) of the mandibular first molars were obtained at a threshold of 270–550 to exclude enamel and distinguish pulp from dentin. The data acquired from the high-resolution scans of four samples per group were used for the quantitative analysis (n = 4).

## Histology analysis

For histologic analyses, the mandibular samples were fixed in freshly prepared 4% PFA in PBS (pH 7.4) at 4 °C overnight and then decalcified in 15% EDTA solution (pH 7.4) at 4 °C for 5–14 days depending on the age of the animals. The samples were embedded in paraffin using standard histological procedures. Serial sections were cut to a thickness of 5 μm and used for Hematoxylin and Eosin (H&E) staining, Toluidine blue staining, immunohistochemistry (IHC), or picro-sirius red staining. To quantify predentin thickness, images were captured under a ×20 objective, the predentin thickness were measured at the cervical region of the first mandibular molars using ImageJ software (n = 3).

For Toluidine blue staining, the mandibular sections were deparaffinized and rehydrated to distilled water and stained in 0.1% Toluidine blue working solution (pH 2.3–2.5) for 2–3 min. Then the sections were washed in distilled water until clear, dehydrated in three changes of 100% ethanol, cleared in xylene and mounted. Toluidine blue is a basic thiazine metachromatic dye that stains background in blue and highlights dentinal tubules in purple.

For the IHC analyses, experiments were carried out using an ABC kit and a DAB kit (Vector Laboratories, Burlingame, CA) according to the manufacturer's instructions. Polyclonal anti-BMP1 antibody (ab118520, Abcam, Cambridge, MA, USA) at a dilution of 1:100 and polyclonal anti-TLL1 antibody (ab107743, Abcam) at a dilution of 1:100 were used to detect the expression pattern of BMP1 and TLL1, respectively. To detect DSP and biglycan, we employed polyclonal antibodies against dentin sialoprotein (DSP, the N-terminal fragment of dentin sialophosphoprotein) at a dilution of 1:2000 and biglycan (LF-159, a gift from Dr. Larry Fisher at the Craniofacial and Skeletal Disease Branch, National Institutes of Health, Bethesda, MD, USA) at a dilution of 1:1000. An affinity-purified polyclonal antibody against periostin at a concentration of 1 μg/ml (Innovative Research, Atlanta, GA, USA) and an affinity-purified polyclonal antibody at a concentration of 20 μg/ml against fibrillin-1 (Sigma-Aldrich, St. Louis, MO, USA) were employed to detect these two ECM molecules in the periodontal ligament (PDL) according to the manufacturers' instructions. The sections were counterstained with methyl green. The same concentrations of normal rabbit IgG were used to replace the polyclonal antibodies serving as negative controls.

For picro-sirius red staining, the sections were immersed in haematoxylin solution for 8 min to stain the nuclei and washed for 10 min in water. Then, the sections were stained in picro-sirius red for 1 h, washed in two changes of acidified water, dehydrated in three changes of 100% ethanol, cleared in xylene and mounted. The structure and organization of the collagen fibers in the dental and periodontal tissues were imaged under polarized light microscope. In the specimens stained by picro-sirius red, the larger collagen fibers were bright yellow or orange, and the thinner ones, including the reticular fibers, appeared green when examined under polarized light.

### Statistical analysis

The quantitative data were expressed as the mean ± SD (standard deviation). The two-group data were analyzed with an unpaired Student's *t* test. $p \leq 0.05$ was considered as the statistically significant difference for all comparisons.

## Results

### Odontoblasts and PDL cells express both *Bmp1* and *Tll1*

X-gal was used to stain the mandibles of $Bmp1^{lacZ\text{-}flox/+}$ mice to reveal the expression of *Bmp1* in the tooth and periodontium (Fig. 2). In the newborn mice, *Bmp1* signals as reflected by the X-gal stain were observed in the odontoblasts and pulp cells in the mandibular first molars (Fig. 2a, b). The alveolar bone surrounding the mandibular first molars also showed positive X-gal staining. In the 5-week-old mice (Fig. 2c, d), strong X-gal stains were seen in the molar odontoblasts, the cells in the periodontal ligament (PDL) and the osteoblasts on the surface of the alveolar bone. Immunohistochemical staining with a polyclonal anti-BMP1 antibody also showed that the odontoblasts and PDL cells express BMP1 (Fig. 2e, f).

X-gal staining showed that the expression level of *Tll1* was lower than *Bmp1* in the dental and periodontal tissues of mice. In the newborn mice, the *Tll1* signals as reflected by the X-

gal stain were barely visible in the odontoblasts or pulp cells of the mandibular first molars (Fig. 3a, b) while very faint signals were observed in the osteoblasts on the surface of alveolar bone surrounding the mandibular first molars. At postnatal 4 weeks, X-gal stains were seen in the odontoblasts and the PDL cells of *Tll1*$^{lacZ\text{-}flox/+}$ mice (Fig. 3c, d). Immunohistochemical staining with a polyclonal anti-Tll1 antibody also showed that mouse odontoblasts express TLL1 (Fig. 3e, f). The expression pattern of X-gal staining and immunohistochemistry showed a certain level of discrepancy, which was likely due to the limited specificity of the anti-TLL1 antibody. The X-gal staining is highly specific and should be considered more accurate in reflecting the expression pattern of the TLL1. Nevertheless, both methods support our conclusion that the odontoblasts express TLL1.

### Loss of *Bmp1* and *Tll1* caused dental defects

In this report, we refer to the *Col1a1*-Cre;*Bmp1*$^{flox/flox}$;*Tll1*$^{flox/flox}$ mice as "double conditional knockout" or "dcKO" mice; in these mice, both *Bmp1* and *Tll1* were inactivated in the Type I collagen-expressing cells. Since the *Bmp1*$^{flox/flox}$ mice, *Tll1*$^{flox/flox}$ mice and *Bmp1*$^{flox/flox}$;*Tll1*$^{flox/flox}$ mice showed completely normal development in either the skeleton or the craniofacial and dental complex, we used these floxed mice (without *Col1a1*-Cre) from the same litters of the dcKO mice as normal controls (Ctrl). We weighed the dcKO mice at different developmental stages and observed that the body size of the dcKO mice was not significantly different from the age- and sex-matched control mice.

During the crossbreeding processes, in addition to the dcKO mice, we also created certain numbers of *Col1a1*-Cre;*Bmp1*$^{flox/+}$;*Tll1*$^{flox/+}$, *Col1a1*-Cre;*Bmp1*$^{flox/flox}$;*Tll1*$^{flox/+}$ and *Col1a1*-Cre;*Tll1*$^{flox/flox}$;*Bmp1*$^{flox/+}$ mice. X-ray radiography analyses showed that the skeletal and dental tissues of *Col1a1*-Cre;*Bmp1*$^{flox/+}$;*Tll1*$^{flox/+}$ mice were completely normal (data not shown), indicating that ablating one allele of *Bmp1* and *Tll1* in the Type I collagen-expressing cells did not cause abnormalities in these tissues. X-ray radiographic examinations revealed that the mandibular first molar and alveolar bone of the *Col1a1*-Cre;*Bmp1*$^{flox/flox}$;*Tll1*$^{flox/+}$ mice had more noticeable defects while those of the *Col1a1*-Cre;*Tll1*$^{flox/flox}$;*Bmp1*$^{flox/+}$ mice did not show obvious abnormalities with the plain X-ray radiography analyses (Fig. 4). The pulp chamber of the mandibular first molar in the *Col1a1*-Cre;*Bmp1*$^{flox/flox}$;*Tll1*$^{flox/+}$ mice was larger than in the normal control mice but appeared smaller than in the *Col1a1*-Cre;*Bmp1*$^{flox/flox}$;*Tll1*$^{flox/flox}$ (dcKO) mice. The alveolar bone in the furcation region between the mesial and distal roots of the mandibular first molar in the *Col1a1*-Cre;*Bmp1*$^{flox/flox}$;*Tll1*$^{flox/+}$ mice had lower radiodensity than in the normal control and a higher radiopacity than in the dcKO mice. In this report, we focus on comparing the dental and periodontal tissues of the dcKO mice vs. those of the normal controls.

Plain X-ray radiography analyses showed that at postnatal 3 weeks, the pulp chambers and root canals of the mandibular first molar in the dcKO mice were larger than in the normal control mice; the molar root was shorter and root dentin thinner in the dcKO mice than in the normal mice (Fig. 5a, b). At postnatal 6 weeks, the defects of the enlarged pulp chamber and reduced dentin thickness in the mandibular first molar of the dcKO mice became more remarkable (Fig. 5c, d). The average length of the mesial root in the first molar of the 6-

week-old control mice was 1.272 ± 0.047 mm while that of the dcKO mice was 1.109 ± 0.087 mm (Fig. 5e). The average dentin thickness at the cervical region in the 6-week-old normal mice was 0.226 ± 0.020 mm while that of the dcKO mice was 0.168 ± 0.015 mm (Fig. 5f).

The μCT analyses were performed on 6-week-old mice to evaluate the structure of the mandible and molars (Fig. 6). The μCT images of the whole mandible at a lower resolution showed that overall, the mineralized tissues did not appear to be significantly different among the four types of mice at 6 weeks (Fig. 6a, c, e, g), while the sagittal sections of 3D reconstructed images confirmed the defects of the enlarged pulp chamber and reduced dentin thickness in the mandibular first molar of the dcKO (Fig. 6d) and *Col1a1-Cre*;*Bmp1*$^{flox/flox}$;*Tll1*$^{flox/+}$ (Fig. 6f) mice. The quantitative analyses of high resolution qCT scans (Fig. 6i–m) revealed that dentin volume of the mandibular first molar (expressed as the ratio of dentin volume to total tooth volume) was significantly lower in dcKO mice compared to Ctrl mice. While the apparent density of dentin in the mandibular first molar was significantly lower in dcKO mice than in Ctrl mice, there was no significant difference in the dentin material density between the two groups.

In summary, both plain X-ray and μCT analyses demonstrated that inactivation of *Bmp1* and *Tll1* in the Type I collagen-expressing cells result in short tooth root, thinner dentin and enlarged pulp chamber in the mandibular first molar.

H&E staining (Fig. 7) analyses showed that the dcKO mice had wider predentin and thinner dentin than the age-matched control mice. Higher magnification views (Fig. 7c, f, i, l) revealed that the odontoblasts were long columnar-shaped in the mandibular first molar of the Ctrl mice, whereas the odontoblasts in the dcKO mice were obviously shorter at postnatal 3 weeks, and became flat or cuboidal at 6 weeks. The average predentin thickness at the cervical region in the first molar of the 6-week-old Ctrl mice was 5.449 ± 0.454 μm, while that of the dcKO mice was 19.397 ± 3.239 μm (Fig. 7m). The predentin of dcKO mice was approximately 2.5 times wider than that of Ctrl mice. Toluidine blue, which stains odontoblast processes, was used to visualize the dentinal tubules in the demineralized sections in this study. Toluidine blue staining (Fig. 8) showed that the dentinal tubules in the molars of the normal mice were well-aligned and evenly distributed, whereas the dentinal tubules in the dcKO mice were disorganized and were fewer in numbers compared to the normal mice.

## Altered levels of biglycan and dentin sialoprotein (DSP) in the predentin-dentin complex of dcKO mice

The immunostaining analyses showed that in the pulp-predentin-dentin complex of normal mice, biglycan was primarily localized in the predentin (Fig. 9a–d). As the molars of the dcKO mice had wider predentin than the control mice, the overall level of biglycan in the former was remarkably greater in the latter mice.

Dentin sialoprotein (DSP) is the N-terminal fragment of dentin sialophosphoprotein (DSPP), the most abundant non-collagenous protein in the predentin-dentin complex. The changes of DSPP level is often associated with altered dentinogenesis. The anti-DSP immunostaining

analyses (Fig. 9e–h) showed that the molar dentin of dcKO mice had less DSP than in the control mice.

### Loss of *Bmp1* and *Tll1* causes periodontal defects

X-ray radiography showed that at postnatal 6 weeks, the alveolar bone in the furcation region of the mandibular first molar and alveolar bone in the interproximal region between the first and second molars of the dcKO mice had reduced radiopacity compared to that of the control mice (Fig. 5d, e). H&E staining (Fig. 10a–h) demonstrated that the distance between the cementoenamel junction and the junctional epithelium (sulcus bottom) in the 6-week-old dcKO mice was similar to that of the control mice, indicating that the dcKO mice did not develop periodontal pockets. The PDL of the dcKO mice did not appear to have more inflammatory cells than the control mice. The picro-sirius red staining (Fig. 11a–h) demonstrated that the collagen fibers in the PDL of the dcKO mice were thicker than the control mice.

### Fibrillin-1 level was reduced in the periodontal ligament of dcKO mice

Periostin and fibrillin-1 are two ECM proteins in the PDL, and the changes in their levels are often associated with PDL defects. The anti-periostin IHC analyses showed that the level of periostin in the PDL of the dcKO mice was similar to that of the control mice (Fig. 12a–d). The antifibrillin-1 immunostaining revealed that the PDL in the dcKO mice had a remarkably lower level of fibrillin-1 compared to the control mice (Fig. 12e–h).

## Discussion

A number of in vitro studies have shown that the four members of the BMP1/tolloid-like family share redundancy in substrate specificity, although their enzyme kinetics such as Vmax and Km values differ (Steiglitz et al. 2004; Hopkins et al. 2007; Von Marschall and Fisher 2010; Muir and Greenspan 2011; Ritchie et al. 2012). While previous studies have shown the co-expression of *Bmp1* and *Tll1* in a variety of tissues including bone (Scott et al. 1999; Muir et al. 2014), there had been no reports about the expression of these activating enzymes in the tooth and periodontal ligament. Data from the present study demonstrated that odontoblast and periodontal ligament cells of the mouse molars expressed both *Bmp1* and *Tll1*, suggesting that the proteinases encoded by these two genes may share redundancy in cleaving and activating proteins secreted into the ECM of the predentin-dentin complex and the PDL. In addition, these proteinases may play essential roles in dentinogenesis and the development of periodontal tissues. Since the titer of the anti-BMP1 antibody may differ from that of the anti-TLL1 antibody, the staining intensity in the IHC analyses with the two types of antibodies may not reflect the actual levels of the proteinases from the two genes. X-gal staining is not only a highly specific approach for detecting the molecules of interest but also avoids the potential issues of binding efficiency variance such as that occurring in the use of different antibodies; thus, the X-gal staining approach is more appropriate for comparing the levels of *Bmp1* and *Tll1* expression. The X-gal staining intensity for *Bmp1* in either the tooth or the periodontium was stronger than that for *Tll1*, indicating that the expression level of the former was higher than the latter. These findings suggest that *Bmp1* may exert a more important role than *Tll1* in the development of dentin and periodontal

ligament. In addition to the dcKO mice, we also generated *Col1a1*-Cre;*Bmp1*$^{flox/flox}$;*Tll1*$^{flox/+}$ mice and *Col1a1*-Cre;*Tll1*$^{flox/flox}$;*Bmp1*$^{flox/+}$ mice but not *Col1a1*-Cre;*Bmp1*$^{flox/flox}$ or *Col1a1*-Cre;*Tll1*$^{flox/flox}$ mice. Future studies are warranted to breed and analyze such mice with the single ablation of either *Bmp1* or *Tll1* (but not both).

Odontoblasts synthesize and secrete a number of ECM proteins (Butler et al. 2002; Qin et al. 2004), some of which are believed to be the substrates of the BMP1/tolloid-like proteinases (Kessler et al. 1996; Li et al. 1996; Steiglitz et al. 2004; Von Marschall and Fisher 2010; Sun et al. 2010; Zhu et al. 2012a; Ritchie et al. 2012). The most abundant protein in the dentin ECM is Type I collagen. *In vitro* studies have shown that BMP1/tolloid-like proteinases cleave and activate Type I procollagen (Kessler et al. 1996; Li et al. 1996). Thus, the speculated cleavage failure of Type I collagen in the dentin or predentin of the dcKO mice might contribute to the dental defects in these mice. The second most prominent protein in the dentin ECM is dentin sialophosphoprotein (DSPP) (Qin et al. 2004). Several in vitro studies have demonstrated that BMP1/tolloid-like proteinases cleave DSPP (Von Marschall and Fisher 2010; Sun et al. 2010; Zhu et al. 2012a; Ritchie et al. 2012). Previously, we showed that the proteolytic processing of DSPP is essential to the formation of a healthy dentin (Zhu et al. 2012b). Therefore, the failure to cleave DSPP may be another major factor responsible for the dentin defects in the dcKO mice. Further studies are needed to determine whether or not DSPP is cleaved in the dentin of the dcKO mice and to examine if the transgenic expression of DSPP fragments can rescue or improve the dentin defects in them.

X-ray radiography analyses showed that dcKO mice underwent alveolar bone loss while histology analyses revealed that these double knockout mice did not develop periodontal pockets at postnatal 6 weeks; these observations indicated that the periodontal disease in these mutant mice was not severe at this age. Picro-sirius red staining showed that the collagen fibers of the PDL in the dcKO mice were thicker than in normal mice, suggesting that the double deletion of *Bmp1* and *Tll1* may have altered the collagen structure of the PDL. The collagen fibers in the PDL are predominantly Type I collagen. BMP1 and TLL1 function as the procollagen carboxy-(C)-proteinases for Type I collagen (Kessler et al. 1996; Hopkins et al. 2007; Muir and Greenspan 2011). The deficiency of BMP1 and TLL1 in the dcKO mice is likely to cause defective proteolytic processing of Type I procollagen and the failure in processing the procollagen may be one of the major factors leading to the abnormal assembly, resulting in the disorganization and thickening of collagen fibers. Transmission electron microscopy analyses showed that the skin of osteogenesis imperfecta patients associated with mutations in the *BMP1* gene had irregular Type I collagen fibers with variable diameters of the fibrils, and some of the fibrils were thicker than the normal controls (Syx et al. 2015). The potential defects in the processing of other ECM molecules such as probiglycan and prolysyl oxidase may also contribute to the collagen abnormality in the PDL of the dcKO mice. While Type I collagen is the most prominent constituent of the PDL and is essential to this tissue, other ECM molecules such as periostin and fibrillin-1 are known to play important roles in the formation and maintenance of a healthy PDL (Rios et al. 2005; Romanos et al. 2014; Shiga et al. 2008; Suda et al. 2009). In this study, we observed a remarkable reduction of fibrillin-1 in the PDL of the dcKO mice. Since the inactivating mutations of fibrillin-1 are associated with periodontal diseases in humans (Shiga et al. 2008; Suda et al. 2009), we speculate that the decreased level of fibrillin-1 may

contribute to the abnormal structure of PDL in the dcKO mice. Fibrillin-1 is synthesized as a precursor (proprotein) known as profibrillin-1 (Milewicz et al. 1992, 1995; Raghunath et al. 1995). It is speculated that profibrillin-1 may be cleaved (activated) into its biologically active form by Furin, a subtilisin-like proprotein convertase that is ubiquitously expressed (Lönnqvist et al. 1998; Raghunath et al. 1999). While we do not have a clear idea about the association between the dramatic reduction of fibrillin-1 and the loss of the BMP1/tolloid-like proteinases in the PDL of the dcKO mice, it is tempting to consider the necessity of testing if these proteinases cleave profibrillin-1.

In summary, our findings in this study suggested that mouse odontoblasts and periodontal ligament cells express both *Bmp1* and *Tll1* and that the proteinases encoded by *Bmp1* and *Tll1* genes play essential roles in the healthy dentin and periodontal ligament. As *Bmp1* and *Tll1* genes are widely expressed, and the conventional deletion of either gene leads to early lethality, the availability of the *Bmp1*- and *Tll1*-floxed mice will allow us to determine their functions in different cell types by using cell-specific Cre-mouse lines. Since the BMP1/tolloid-like proteinases cleave a number of secretory proteins, future studies are needed to examine which secretory proteins may be affected in the mouse tissues lacking *Bmp1* and *Tll1* genes.

## Acknowledgements

This work was supported by the United States National Institutes of Health Grants DE022549 and DE023365. We thank Jeanne Santa Cruz for her assistance with the editing of this article.

## References

Butler WT, Brunn JC, Qin C, McKee MD (2002) Extracellular matrix proteins and the dynamics of dentin formation. Connect Tissue Res 43:301–307 [PubMed: 12489174]

Clark TG, Conway SJ, Scott IC, Labosky PA, Winnier G, Bundy J, Hogan BL, Greenspan DS (1999) The mammalian Tolloid-like 1 gene, Tll1, is necessary for normal septation and positioning of the heart. Development 126:2631–2642 [PubMed: 10331975]

Hopkins DR, Keles S, Greenspan DS (2007) The bone morphogenetic protein 1/Tolloid-like metalloproteinases. Matrix Biol 26:508–523 [PubMed: 17560775]

Kessler E, Takahara K, Biniaminov L, Brusel M, Greenspan DS (1996) Bone morphogenetic protein-1: the type I procollagen C-proteinase. Science 271:360–362 [PubMed: 8553073]

Lee SJ (2008) Genetic analysis of the role of proteolysis in the activation of latent myostatin. Plos One 3:e1628 [PubMed: 18286185]

Leighton M, Kadler KE (2003) Paired basic/furin-like proprotein convertase cleavage of pro-BMP-1 in the trans-Golgi network. J Biol Chem 278:18478–18484 [PubMed: 12637569]

Li R, Zhang Q (2015) HtrA1 may regulate the osteogenic differentiation of human periodontal ligament cells by TGF-βE J Mol Histol 46(2):137–144 [PubMed: 25726184]

Li SW, Sieron AL, Fertala A, Hojima Y, Arnold WV, Prockop DJ (1996) The C-proteinase that processes procollagens to fibrillar collagens is identical to the protein previously identified as bone morphogenic protein-1. Proc Natl Acad Sci USA 93:5127–5130 [PubMed: 8643539]

Liu P, Zhang H, Liu C, Wang X, Chen L, Qin C (2014) Inactivation of Fam20C in cells expressing type I collagen causes periodontal disease in mice. PLoS One 9:e114396 [PubMed: 25479552]

Lönnqvist L, Reinhardt D, Sakai L, Peltonen L (1998) Evidence for furin-type activity-mediated C-terminal processing of profibrillin-1 and interference in the processing by certain mutations. Hum Mol Genet 13:2039–2044

Milewicz DM, Pyeritz RE, Crawford ES, Byers PH (1992) Marfan syndrome: defective synthesis, secretion and extracellular matrix formation of fibrillin by cultured dermal fibroblasts. J Clin Invest 89:79–86 [PubMed: 1729284]

Milewicz DM, Grossfield J, Cao S-N, Kielty C, Covitz W, Jewett T (1995) A mutation in FBN1 disrupts profibrillin processing and results in isolated skeletal features of the Marfan syndrome. J Clin Invest 95:2373–2378 [PubMed: 7738200]

Muir A, Greenspan DS (2011) Metalloproteinases in *Drosophila* to humans that are central players in developmental processes. J Biol Chem 286:21911–41905

Muir AM, Ren Y, Butz DH, Davis NA, Blank RD, Birk DE, Lee SJ, Rowe D, Feng JQ, Greenspan DS (2014) Induced ablation of Bmp1 and Tll1 produces osteogenesis imperfecta in mice. Hum Mol Genet 23:3085–3101 [PubMed: 24419319]

Muromachi K, Kamio N, Matsuki-Fukushima M, Nishimura H, Tani-Ishii N, Sugiya H, Matsushima K (2015) CCN2/CTGF expression via cellular uptake of BMP-1 is associated with reparative dentinogenesis. Oral Dis 21:778–784 [PubMed: 25944709]

Qin C, Baba O, Butler WT (2004) Posttranslational modifications of SIBLING proteins and their roles in osteogenesis and dentinogenesis. Crit Rev Oral Biol Med 15:126–136 [PubMed: 15187031]

Raghunath M, Kielty CM, Steinmann B (1995) Truncated profibrillin of a Marfan patient is of apparent similar size as fibrillin: intracellular retention leads to over-N-glycosylation. J Mol Biol 248:901–909 [PubMed: 7760331]

Raghunath M, Putnam EA, Ritty T, Hamstra D, Park ES, Tschödrich-Rotter M, Peters R, Rehemtulla A, Milewicz DM (1999) Carboxy-terminal conversion of profibrillin to fibrillin at a basic site by PACE/furin-like activity required for incorporation in the matrix. J Cell Sci 112:1093–1100 [PubMed: 10198291]

Reynolds SD, Zhang D, Puzas JE, O'Keefe RJ, Rosier RN, Reynolds PR (2000) Cloning of the chick BMP1/Tolloid cDNA and expression in skeletal tissues. Gene 248:233–243 [PubMed: 10806368]

Rios H, Koushik SV, Wang H, Wang J, Zhou HM et al. (2005) Periostin null mice exhibit dwarfism, incisor enamel defects, and an early-onset periodontal disease-like phenotype. Mol Cell Biol 25:11131–11144 [PubMed: 16314533]

Ritchie HH, Yee CT, Tang XN, Dong Z, Fuller RS (2012) DSP-PP precursor protein cleavage by tolloid-related-1 protein and by bone morphogenetic protein-1. PLoS One 7:e41110 [PubMed: 22815932]

Romanos GE, Asnani KP, Hingorani D, Deshmukh VL (2014) Periostin: role in formation and maintenance of dental tissues. J Cell Physiol 229:1–5 [PubMed: 23702840]

Scott IC, Blitz IL, Pappano WN, Imamura Y, Clark TG, Steiglitz BM, Thomas CL, Maas SA, Takahara K, Cho KW, Greenspan DS (1999) Mammalian BMP-1/tolloid-related metalloproteinases, including novel family member mammalian tolloid-like 2, have differential enzymatic activities and distributions of expression relevant to patterning and skeletogenesis. Dev Biol 213:283–300 [PubMed: 10479448]

Shiga M, Saito M, Hattori M, Torii C, Kosaki K et al. (2008) Characteristic phenotype of immortalized periodontal cells isolated from a Marfan syndrome type I patient. Cell Tissue Res 331:461–472 [PubMed: 18049824]

Steiglitz BM, Ayala M, Narayanan K, George A, Greenspan DS (2004) Bone morphogenetic protein-1/Tolloid-like proteinases process dentin matrix protein-1. J Biol Chem 279:980–986 [PubMed: 14578349]

Sterchi EE, Stöcker W, Bond JS (2008) Meprins, membrane-bound and secreted astacin metalloproteinases. Mol Aspects Med 29:309–328 [PubMed: 18783725]

Suda N, Shiga M, Ganburged G, Moriyama K (2009) Marfan syndrome and its disorder in periodontal tissues. J Exp Zool B Mol Dev Evol 312B:503–509 [PubMed: 19199346]

Sun Y, Lu Y, Chen S, Prasad M, Wang X, Zhu Q, Zhang J, Ball H, Feng J, Butler WT, Qin C (2010) Key proteolytic cleavage site and full-length form of DSPP. J Dent Res 89:498–503 [PubMed: 20332332]

Suzuki N, Labosky PA, Furuta Y, Hargett L, Dunn R, Fogo AB, Takahara K, Peters DM, Greenspan DS, Hogan BL (1996) Failure of ventral body wall closure in mouse embryos lacking a

procollagen C-proteinase encoded by Bmp1, a mammalian gene related to *Drosophila* tolloid. Development 122:3587–3595 [PubMed: 8951074]

Syx D, Guillemyn B, Symoens S, Sousa AB, Medeira A, Whiteford M, Hermanns-Lê T, Coucke PJ, De Paepe A, Malfait F (2015) Defective proteolytic processing of fibrillar procollagens and prodecorin due to biallelic BMP1 mutations results in a severe, progressive form of osteogenesis imperfecta. J Bone Miner Res 30:1445–1456 [PubMed: 25656619]

Takahara K, Lyons GE, Greenspan DS (1994) Bone morphogenetic protein-1 and a mammalian tolloid homologue (mTld) are encoded by alternatively spliced transcripts which are differentially expressed in some tissues. J Biol Chem 269:32572–32578 [PubMed: 7798260]

Tsuchiya S, Simmer JP, Hu JC, Richardson AS, Yamakoshi F, Yamakoshi Y (2011) Astacin proteases cleave dentin sialophosphoprotein (Dspp) to generate dentin phosphoprotein (Dpp). J Bone Miner Res 2011:220–228

Von Marschall Z, Fisher LW (2010) Dentin sialophosphoprotein (DSPP) is cleaved into its two natural dentin matrix products by three isoforms of bone morphogenetic protein-1 (BMP1). Matrix Biol 29:295–303 [PubMed: 20079836]

Yang G, Jiang B, Cai W, Liu S, Zhao S (2016) Hyaluronan and hyaluronan synthases expression and localization in embryonic mouse molars. J Mol Histol 47(4):413–420 [PubMed: 27318667]

Ye X, Zhang J, Yang P (2016) Hyperlipidemia induced by high-fat diet enhances dentin formation and delays dentin mineralization in mouse incisor. J Mol Histol 47(5):467–474 [PubMed: 27558143]

Zhou Z, Yin Y, Jiang F, Niu Y, Wan S, Chen N, Shen M (2016) CBX7 deficiency plays a positive role in dentin and alveolar bone development. J Mol Histol 47(4):401–411 [PubMed: 27271093]

Zhu Q, Prasad M, Kong H, Lu Y, Sun Y, Wang X, Yamoah A, Feng JQ, Qin C (2012a) Partial blocking of mouse DSPP processing by substitution of $Gly^{451}$-$Asp^{452}$ bond suggests the presence of secondary cleavage site(s). Connect Tissue Res 53:307–312 [PubMed: 22175728]

Zhu Q, Gibson MP, Liu Q, Liu Y, Lu Y, Wang X, Feng JQ, Qin C (2012b) Proteolytic processing of dentin sialophosphoprotein (DSPP) is essential to dentinogenesis. J Biol Chem 287:30426–30435 [PubMed: 22798071]

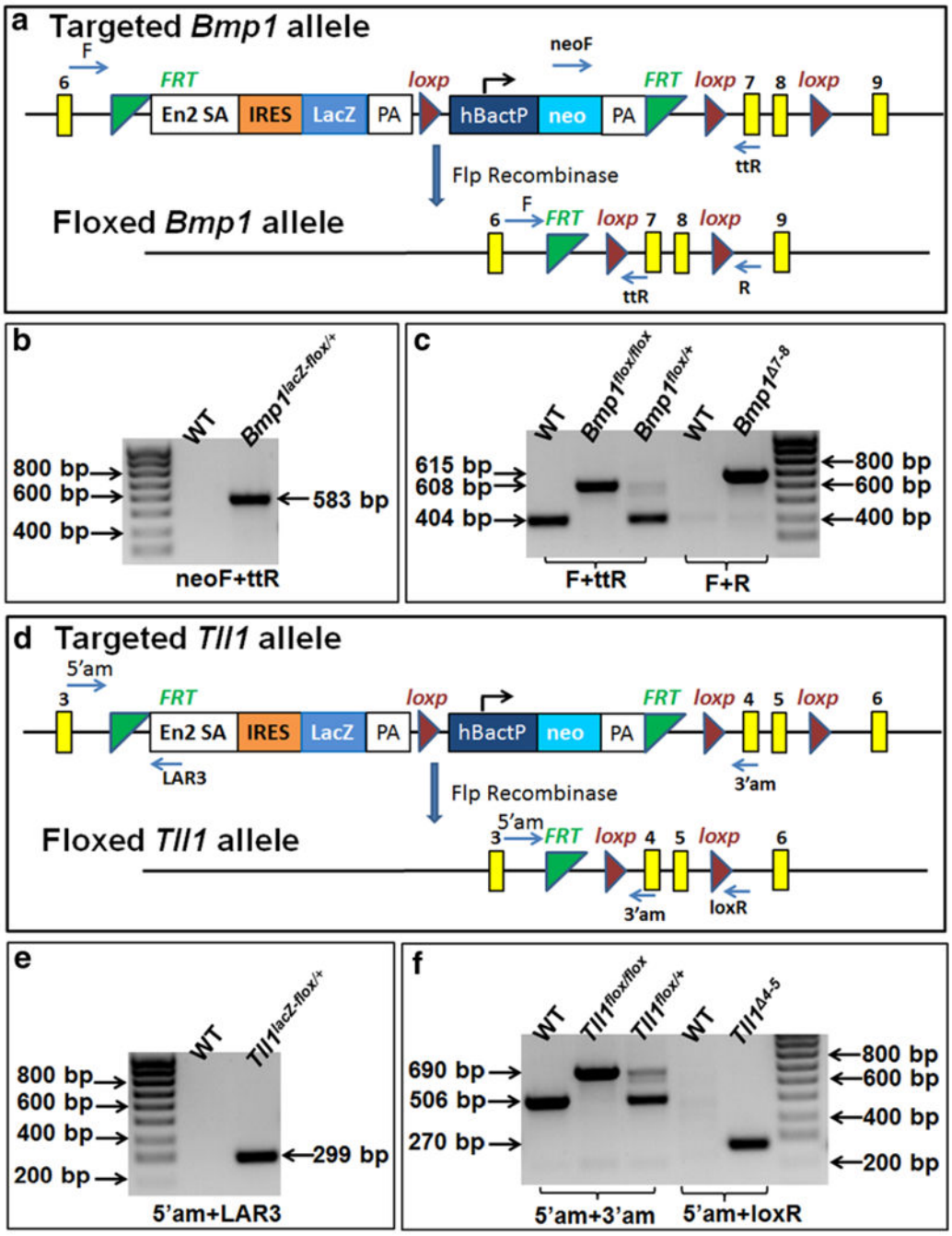


**Fig. 1.**

Generation of *Bmp1* and *Tll1* floxed alleles, and genotyping strategy. **a** Targeted and floxed *Bmp1* allele. An IRES-lacZ-Neo cassette flanked by two flippase recognition target (FRT) sites (*green triangle*) was inserted into intron 6; the region of exons 7 and 8 was flanked by two loxP sites (*red triangle*). Recombination after Flp recombinase scission would remove the IRES-lacZ-Neo cassette from targeted *Bmp1* allele and generate floxed *Bmp1* allele. **b** We used the primer set of neoF and ttR to identify the $Bmp1^{lacZ\text{-}flox}$ allele. PCR with this set of primers produced a 583 bp fragment from the $Bmp1^{lacZ\text{-}flox}$ allele. **c** We used the primer

set of F and ttR to distinguish the floxed allele from the wild type (WT) allele. *Bmp1*-ablated (*Bmp1*$^{\Delta 7\text{-}8}$) allele after Cre-loxP recombination was identified by the primer set of F and R; PCR with this set of primers generated a 615 bp fragment from the *Bmp1*$^{\Delta 7\text{-}8}$ allele. **d** Targeted and floxed *Tll1* allele. An IRES-lacZ-Neo cassette flanked by two FRT sites was inserted into intron 3; the region of exons 4 and 5 was flanked by two loxP sites. Recombination after Flp recombinase scission would remove the IRES-lacZ-Neo cassette from the targeted *Tll1* allele and generate the floxed *Tll1* allele. **e** We used the primer set of 5′am and FAR3 to identify the *Tll1*$^{lacZ\text{-}flox}$ allele; PCR with these primers produced a 299 bp fragment from the *Tll1*$^{lacZ\text{-}flox}$ allele. **f** We used the primer set of 5′am and 3′am to distinguish the floxed allele from the wild type (WT) allele. *Tll1*-ablated (*Tll1*$^{\Delta 4\text{-}5}$) allele after cre-loxP recombination was identified by the primer set of F and R; PCR with theses primers generated a 615 bp fragment from the *Tll1*$^{\Delta 4\text{-}5}$ allele. (Color figure online)

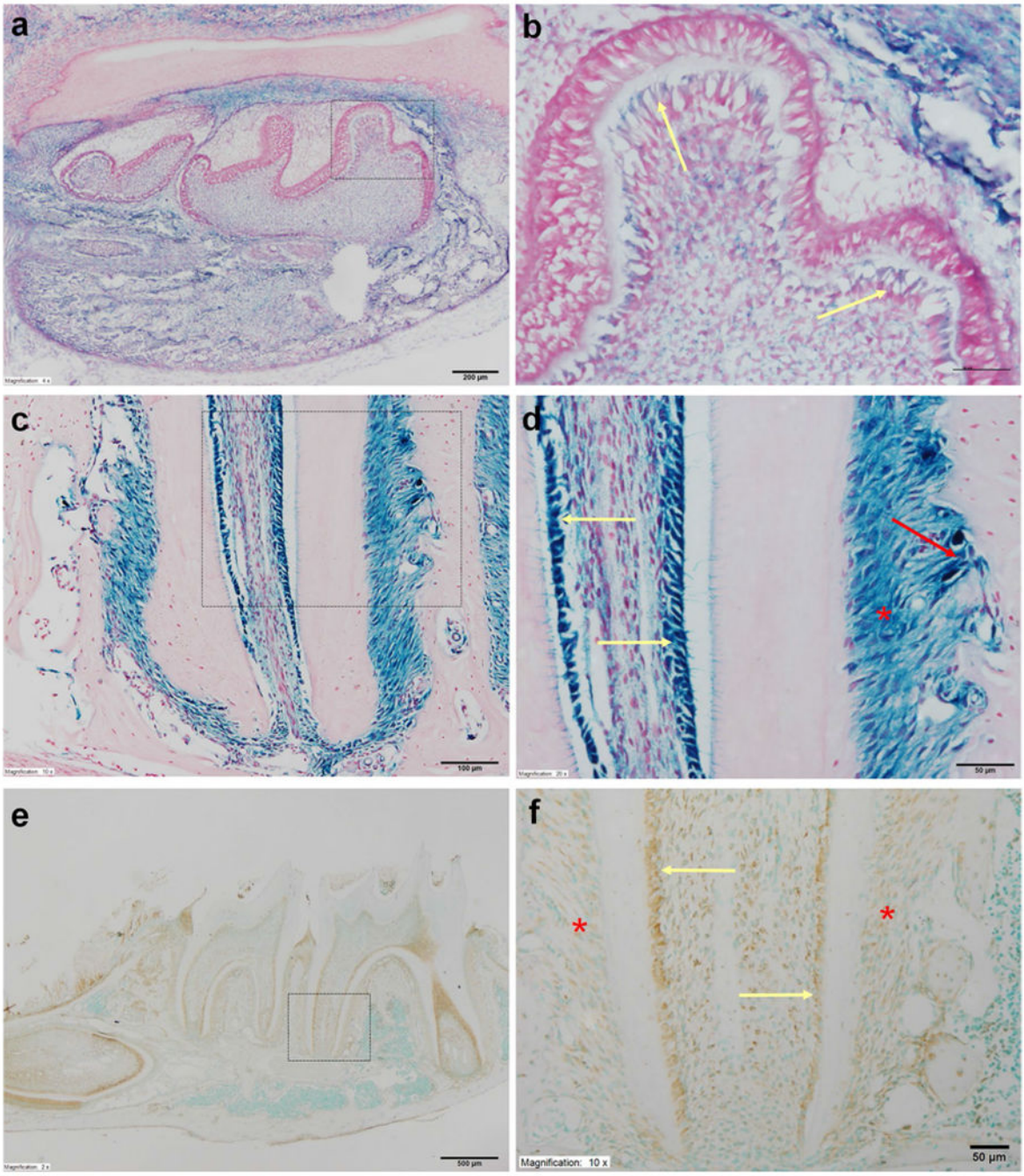


**Fig. 2.**

Expression of *Bmp1* in the mouse dental and periodontal tissues. **a** X-gal staining of the mandible in the newborn (NB) *Bmp1*$^{lacZ\text{-}flox/+}$ mice. Note the strong *Bmp1* signals in the mandibular molars and the surrounding alveolar bone, as reflected by the X-gal staining. *Scale bar* 200 µm. **b** Higher magnification view of the box area in **a**. *Bmp1* signals were present in the odontoblasts (*yellow arrows*). *Scale bar* 50 µm. **c** X-gal staining for the root region of the mandibular first molar in the 5-week-old *Bmp1*$^{lacZ\text{-}flox/+}$ mice. The imaging of this region allowed us to simultaneously observe and compare the galactosidase activities in

the three types of cells: odontoblasts, bony cells and PDL cells. *Scale bar* 200 μm. **d** Higher magnification view of the box area in **c**. Strong *Bmp1* signals were observed in the odontoblasts (*yellow arrows*), osteoblasts (*red arrow*) and cells in the periodontal ligament (PDL) (*red asterisk*). *Scale bar* 100 μm. **e** Immunohistochemical staining of BMP1 for the mandible of 3-week-old mice. *Scale bar* 500 μm. **f** Higher magnification view of the box area in **e** showed that both odontoblasts (*yellow arrows*) and PDL cells (*red asterisks*) express BMP1. *Scale bar* 50 μm. (Color figure online)

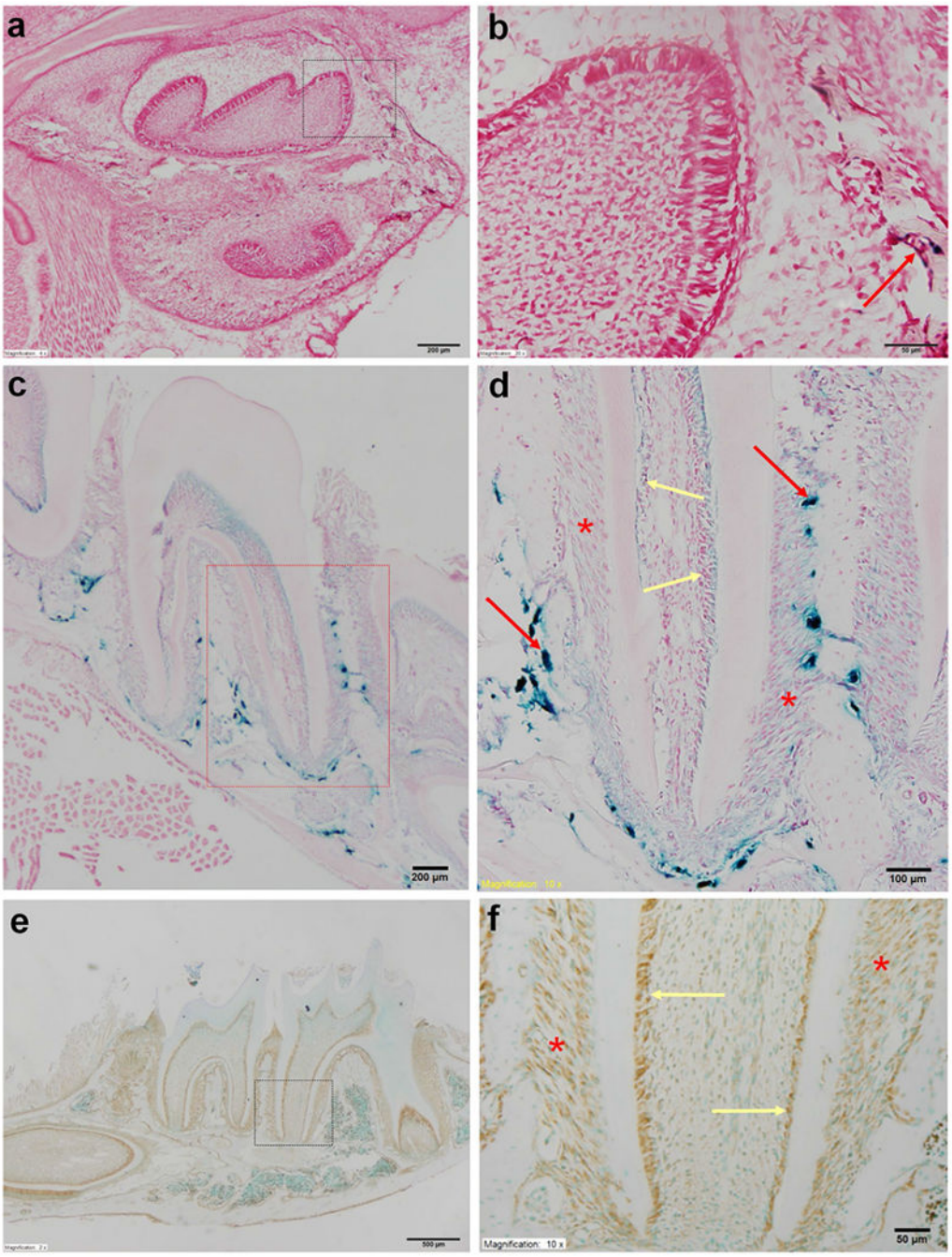


**Fig. 3.**

Expression of *Tll1* in the mouse dental and periodontal tissues. **a** X-gal staining of the mandible in the newborn (NB) $Tll1^{lacZ\text{-}flox/+}$ mice. The *Tll1* signals were weakly positive in the alveolar bone surrounding the mandibular first molar and incisor. *Scale bar* 200 μm. **b** Higher magnification view of the box area revealed that the *Tll1* signals were hardly detectable in the molar odontoblasts (*yellow arrows*) of the NB mouse. *Scale bar* 50 μm. **c** X-gal staining of the mandibular molars in the 4-week-old $Tll1^{lacZ\text{-}flox}$ mice. *Scale bar* 200 μm. **d** Higher magnification view of the box area in **c**. *Tll1* signals were relatively strong in

the osteoblasts (*red arrows*), but weak in the odontoblasts (*yellow arrows*) and PDL cells (*red asterisks*). *Scale bar* 100 μm. **e** Immunohistochemical staining of TLL1 in the mandible of 3-week-old mice. *Scale bar* 500 μm. **f** Higher magnification view of the box area in **e** showed that both odontoblasts (*yellow arrows*) and PDL cells (*red asterisks*) expressed TLL1. *Scale bar* 50 μm. (Color figure online)

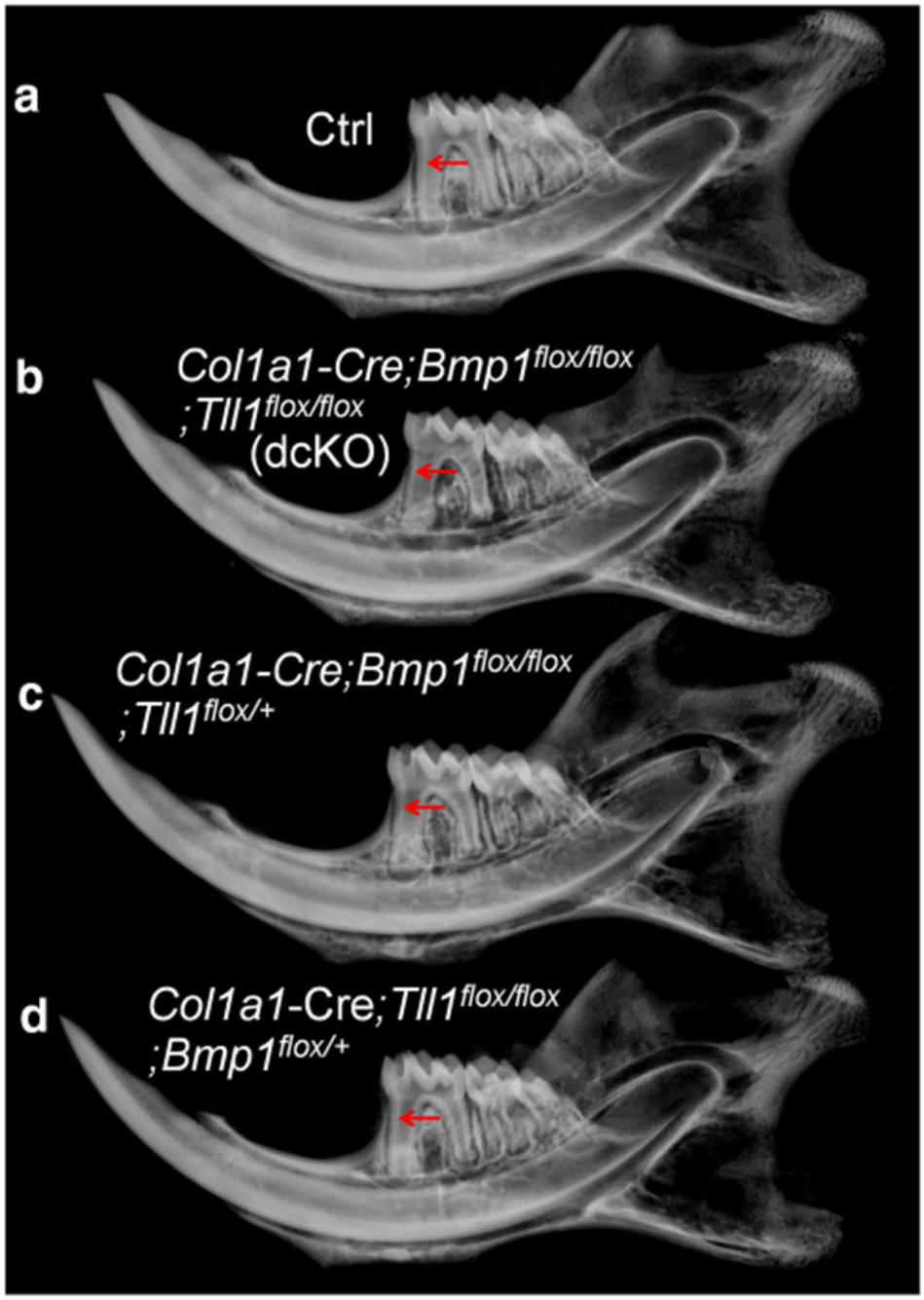


**Fig. 4.**

X-ray radiography analyses of the normal control (Ctrl), *Col1a1*-Cre;*Bmp1*$^{flox/flox}$;*Tll1*$^{flox/flox}$ (double conditional knockout, dcKO), *Col1a1*-Cre;*Bmp1*$^{flox/flox}$;*Tll1*$^{flox/+}$ and *Col1a1*-Cre;*Tll1*$^{flox/flox}$;*Bmp1*$^{flox/+}$ mice. Compared to the normal control (Ctrl) mice (**a**), the mandibular first molar of the dcKO (**b**) and *Col1a1*-Cre;*Bmp1*$^{flox/flox}$;*Tll1*$^{flox/+}$ mice (**c**) displayed thinner dentin, enlarged pulp chambers and obvious bone loss in the alveolar bone; while the mandibular first molar of *Col1a1*-

Cre;*Tll1*$^{flox/flox}$;*Bmp1*$^{flox/+}$ mice (**d**) did not show obvious difference compared with the Ctrl mice (**a**)

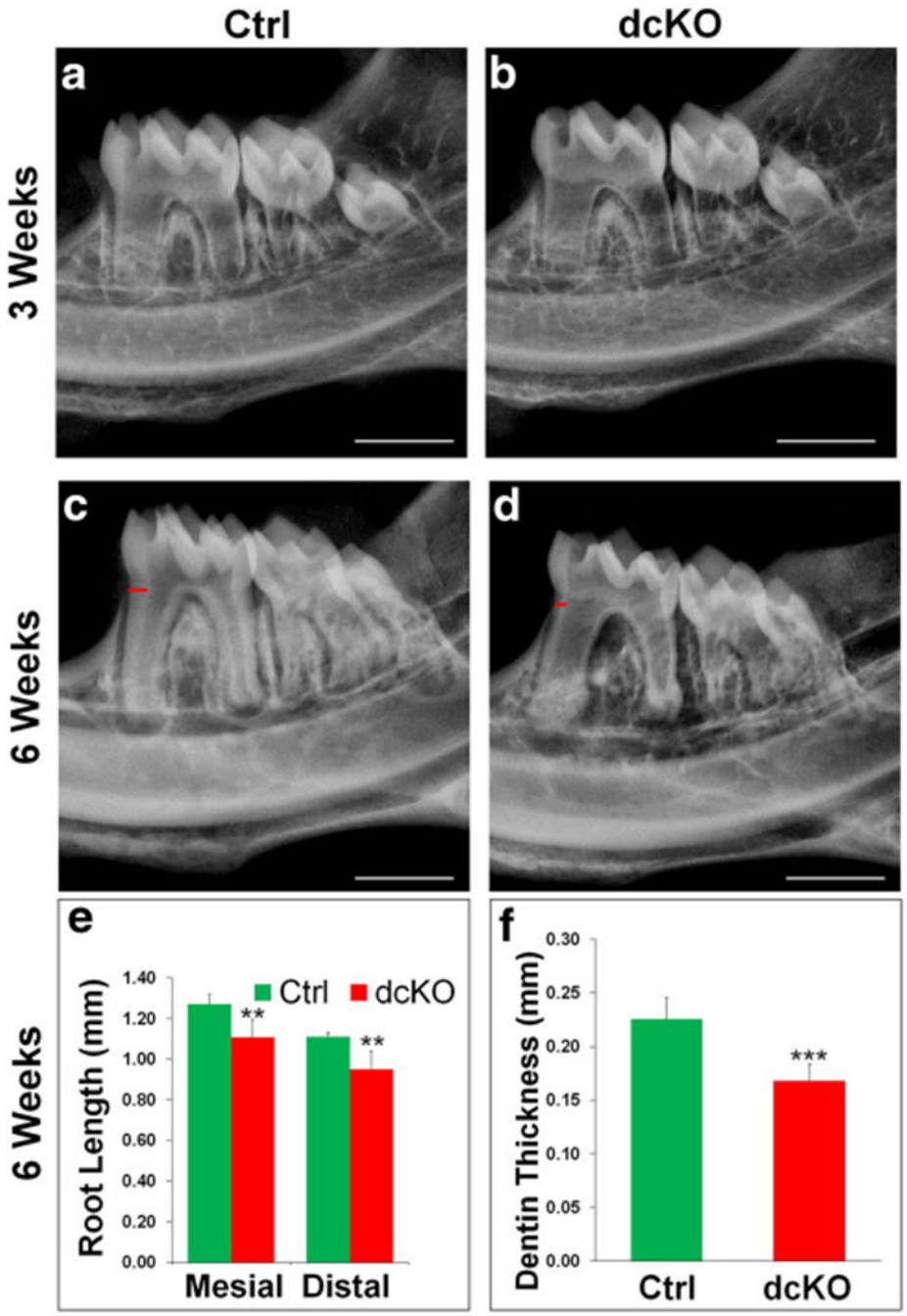


**Fig. 5.**

X-ray radiography analyses of *Col1a1*-Cre;*Bmp1*$^{flox/flox}$;*Tll1*$^{flox/flox}$ (dcKO) mice. At 3 weeks (**a, b**), the mandibular teeth (molars and incisors) of dcKO mice (**b**) showed slightly thinner dentin and larger pulp chambers than the control mice (**a**). At 6 weeks, the dcKO (**d**) displayed markedly reduced dentin thickness, accompanied by a larger pulp chamber, shorter roots and reduced radiopacity in the alveolar bone. The measurement of the mesial and distal root lengths of the first molars revealed a ~13% reduction in the mesial root length and ~14% decreases in the distal root (**e**). In addition, the dentin thickness of dcKO mice

showed a 25.4% reduction compared with the control mice (**f**). Data are presented as the mean ± SD (n = 5). **p < 0.01, ***p < 0.001. *Scale bars* (*white*) in **a–c** and **d** = 1 mm. *Red bars* in **c** and **d** indicated the regions of the teeth that were used to measure the dentin thickness. (Color figure online)

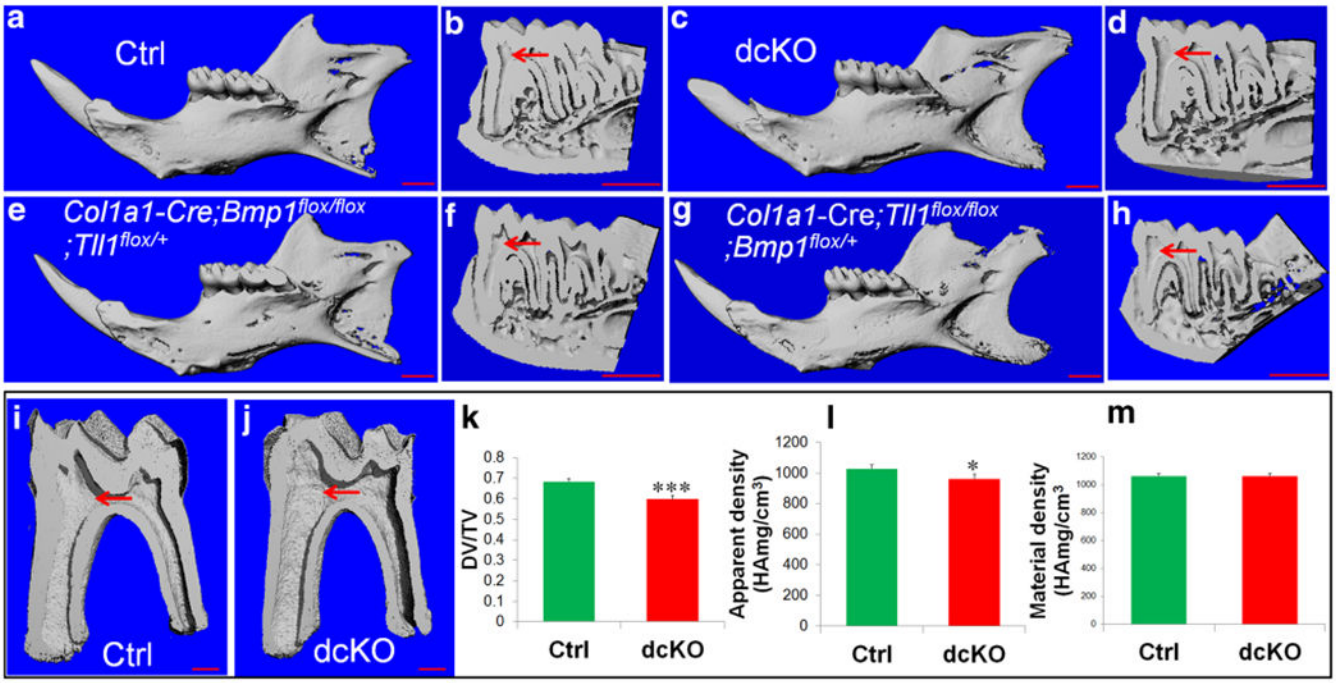


**Fig. 6.**

The $\mu$CT analyses of mandibles from 6-week-old mice. Representative $\mu$CT images of mandibles from 6-week old Ctrl (**a, b**), dcKO (**c, d**), *Col1a1*-Cre;*Bmp1*$^{flox/flox}$;*Tll1*$^{flox/+}$ (**e, f**) and *Col1a1*-Cre;*Tll1*$^{flox/flox}$;*Bmp1*$^{flox/+}$ (**g, h**) mice. *Scale bars* 1.0 mm in **a–h. i, j** The representative μCT images (3D reconstruction) of mandibular first molars in the Ctrl and dcKO mice. *Scale bars* 500 μm in **i** and **j**. Quantitative analyses demonstrating significantly reduced dentin volume and apparent density in dcKO mice, compared to the Ctrl mice. Values of dentin volume are expressed as a ratio of dentin volume (DV) to total tissue volume (TV), where the TV is a sum of the dentin and pulp volume. There was not significant difference in dentin mineral density between the two groups. Data are presented as the mean ± SD (n = 4). *p < 0.05, ***p < 0.001

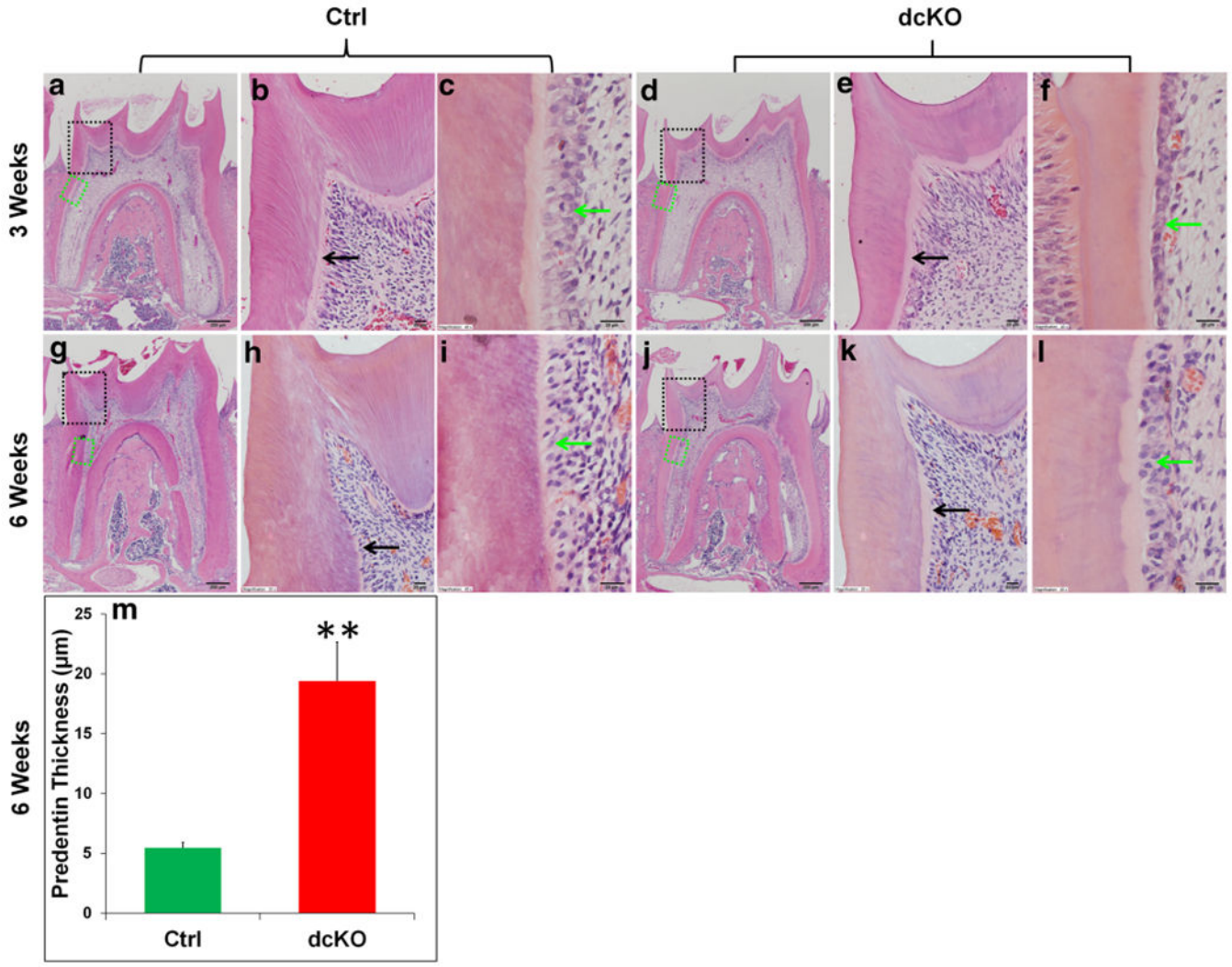


**Fig. 7.**

H&E staining analyses of the mandibular first molars in dcKO mice. **b, c** The higher magnification views of the *black* and *green box* areas in **a**, respectively. **e, f** The higher magnification views of the *black* and *green box* areas in **d. h, i** The higher magnification views of the *black* and *green box* areas in **g. k, l** The higher magnification views of the *black* and *green box* areas in **j**. At both 3 weeks (**a–f**) and 6 weeks (**g–l**) of age, dcKO mice showed thinner dentin, widened predentin zone (*black arrows*) and deformed odontoblasts (*green arrows*). *Scale bars* 200 μm (**a, d, g, j**) and 20 μm (**b, c, e, f, h, i, k, l**). The predentin width of the dcKO mice was 2.5 times of that in the Ctrl mice (**m**). Data are presented as the mean ± SD (n = 3). **p < 0.01. (Color figure online)

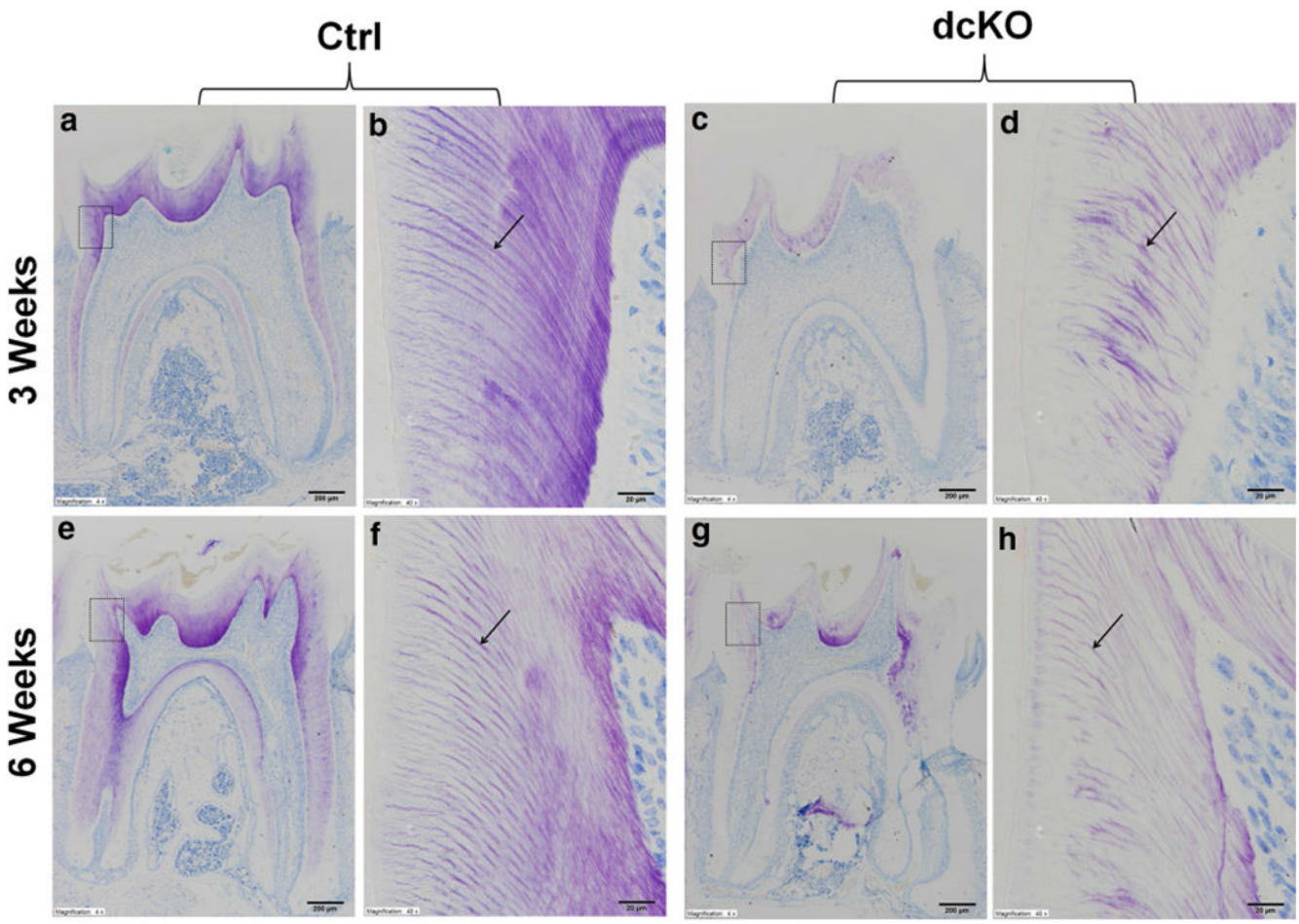


**Fig. 8.**

Toluidine blue staining analyses of the mandibular first molars in dcKO mice. **b** The higher magnification view of the box area in **a. d** The higher magnification view of the box area in **c. f** The higher magnification view of the box area in **e. h** The higher magnification view of the box area in **g**. Toluidine *blue* highlighted the dentinal tubules (*black arrows*) in *purple color*. At both 3 weeks (**a–d**) and 6 weeks (**e–h**) of ages, the dentinal tubule structure was poorly formed, disorganized and dramatically reduced in number in dcKO mice. *Scale bars* 200 μm (**a, c, e, g**) and 20 μm (**b, d, f, h**). (Color figure online)

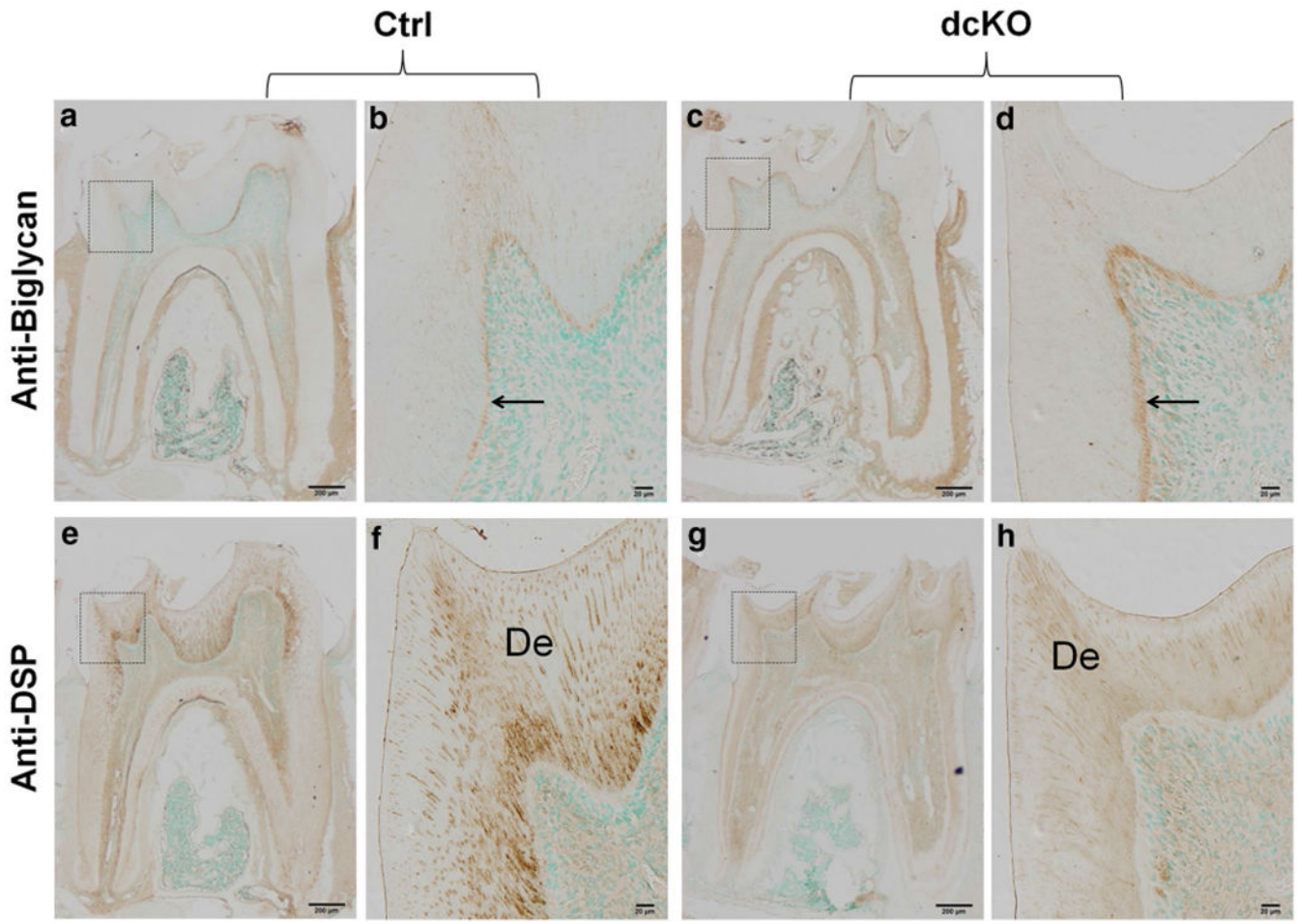


**Fig. 9.**

IHC analyses of the mandibular first molars in dcKO mice. **b** The higher magnification view of the box area in **a. d** The higher magnification view of the box area in **c. f** The higher magnification view of the box area in **e. h** The higher magnification view of the box area in **g. a–d** Biglycan immunostaining of the mandibular first molars from 6-week-old ctrl (**a, b**) and dcKO (**c, d**) mice. Note that biglycan signals (*brown color*) were primarily restricted to the predentin zone (*black arrows*). The dcKO mice displayed a widened zone and a higher level of biglycan immunostaining signals compared with the Ctrl mice. **e–h** Immunohistochemical detection of DSP (*brown color*) in the mandibular first molars from 6-week-old Ctrl (**e, f**) and dcKO (**g, h**) mice. The signals were markedly reduced and unevenly distributed in the dentin matrix of the dcKO mice. *De* dentin. *Scale bars* 200 μm (**a, c, e, g**) and 20 μm (**b, d, f, h**). (Color figure online)

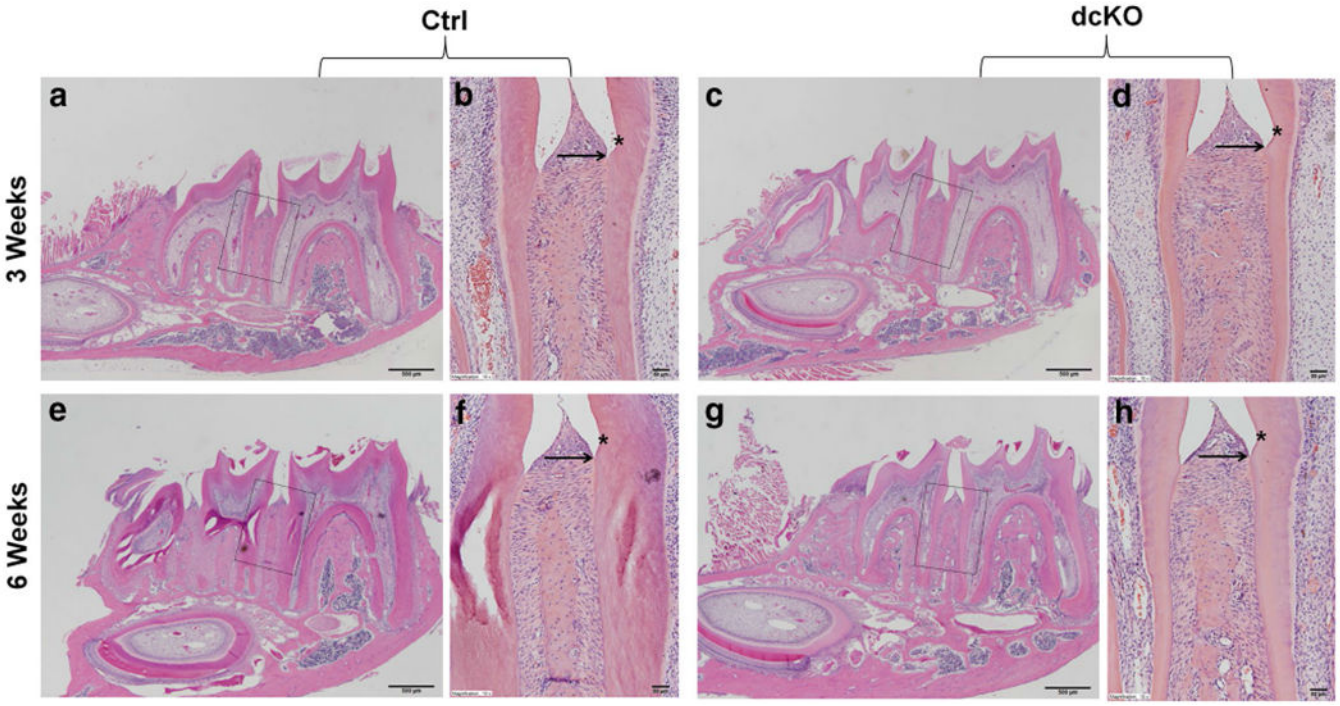


**Fig. 10.**

H&E staining analyses of periodontal tissues in dcKO mice. b The higher magnification view of the box area in **a. d** The higher magnification view of the box area in **c. f** The higher magnification view of the box area in **e. h** The higher magnification view of the box area in **g**. *Asterisks* indicate the cemento-enamal junctions. *Black arrows* indicated the sulcus bottom. At 3 weeks (**a–d**) and 6 weeks (**e–h**), the height and area of alveolar bone in the interdental regions of the dcKO mice (**d, h**) were similar to those of the normal mice (**b, f**), and PDL had no significant inflammation. *Scale bars* 500 μm (**a, c, e, g**) and 50 μm (**b, d, f, h**)

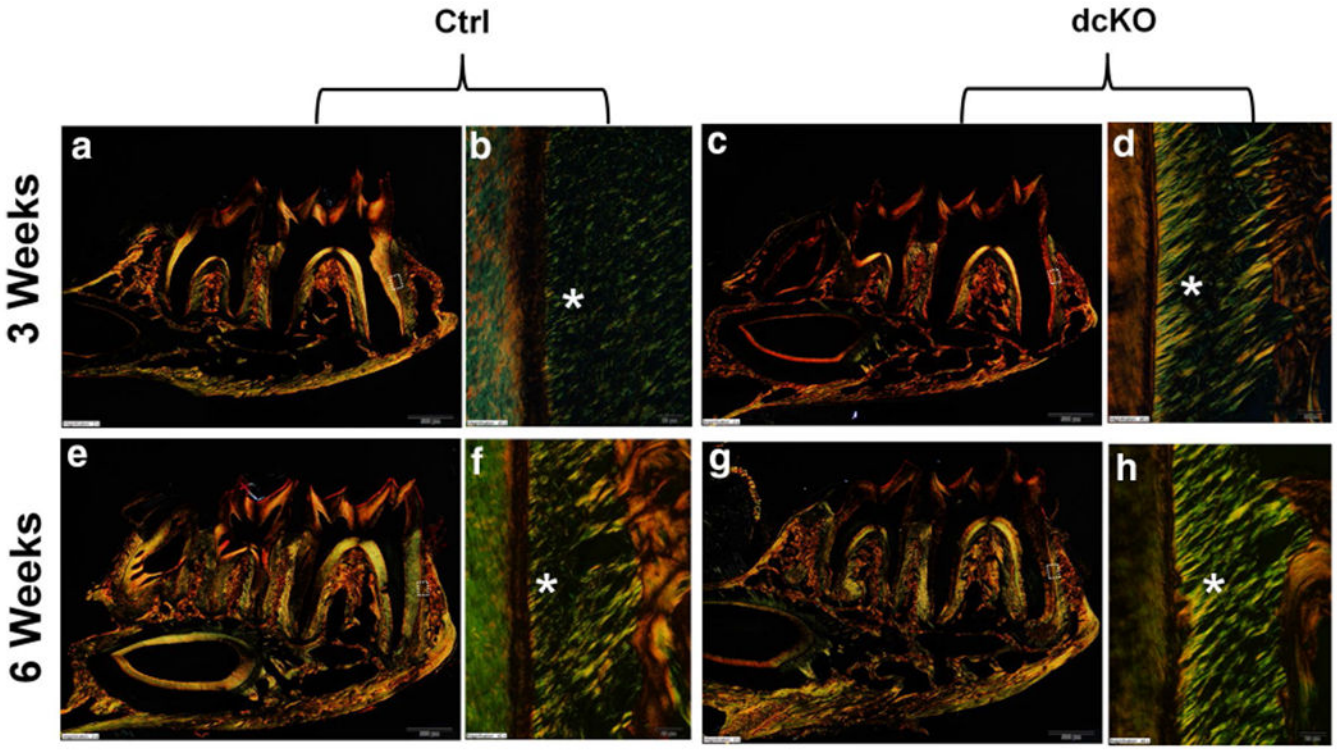


**Fig. 11.**

Picro-sirius red staining analyses of periodontal tissues in dcKO mice. **b** The higher magnification view of the box area in **a. d** The higher magnification view of the box area in **c. f** The higher magnification view of the box area in **e. h** The higher magnification view of the box area in **g**. *Bright yellow* or *orange color* indicates larger (thicker) collagen fibers, whereas *green color* implies thinner collagen fibers. At both 3 weeks and 6 weeks, a large amount of thicker collagen fibers were found in the PDL of the dcKO mice (**d, h**). *Scale bars* 500 μm (**a, c, e, g**) and 20 μm (**b, d, f, h**). (Color figure online)

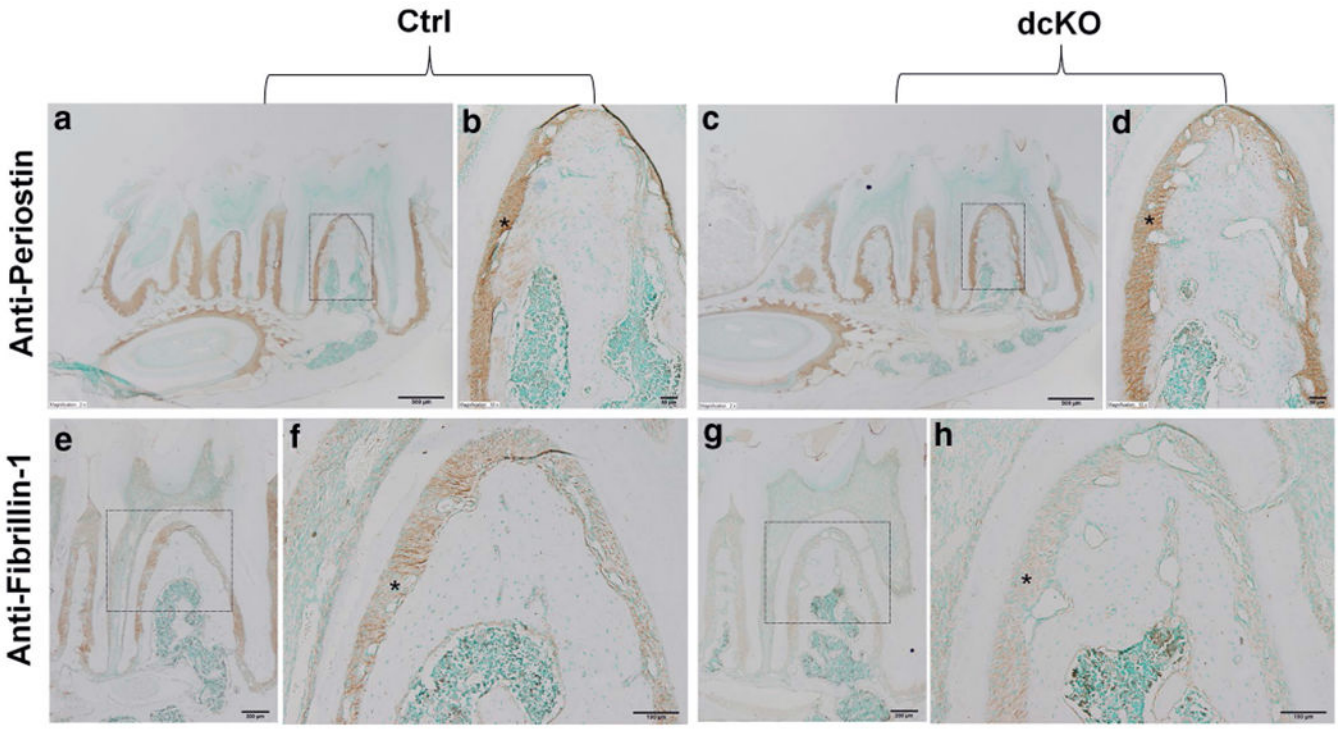


**Fig. 12.**

IHC analyses of periodontal tissues in 6-week-old mice. **b** The higher magnification view of the box area in **a. d** The higher magnification view of the box area in **c. f** The higher magnification view of the box area in **e. h** The higher magnification view of the box area in **g**. Strong signals for periostin were seen in the PDL in both Ctrl (**a, b**) and dcKO (**c, d**) mice at a similar staining level. Fibrillin-1 was also expressed in PDL and its signals were dramatically weaker in the PDL of dcKO mice (**g, h**) compared to the Ctrl mice (**e, f**). *Asterisks* indicated PDL. *Scale bars* 500 μm (**a, c**), 200 μm (**e, g**), 50 μm (**f, h**) and 20 μm (**b, d**)

**Table 1**

Primers used for genotyping

| Name | Sequence (5′–3′) |
|---|---|
| BMP1-neoF | GGGATCTCATGCTGGAGTTCTTCG |
| BMP1-ttR | TTATGCTCAGACTGGCTTCAAACCG |
| BMP1-F | CCCACAGACCCTCCTTCTATTTCCC |
| BMP1-R | TGCTTTGTTCTCAGCTGTTCTCAGG |
| Tll1-5′am | CTGATAGCTGGATGCTAGCACAGG |
| Tll1-LAR3 | CAACGGGTTCTTCTGTTAGTCC |
| Tll1-3′am | GAAGTCCTCAGTCAGAGTCATATACC |
| Tll1-loxR | TGAACTGATGGCGAGCTCAGACC |